Heliyon 5 (2019) e01703

Contents lists available at ScienceDirect

Heliyon

journal homepage: www.heliyon.com

Synthesis and radiation shielding properties of polyimide/Bi_2O_3 composites

V.I. Pavlenko, N.I. Cherkashina *, R.N. Yastrebinsky

Institute of Chemical Technology, Radiation Monitoring Laboratory, Belgorod State Technological University Named After V.G. Shoukhov, Belgorod, 308012, Kostyukov str., 46, Russia

ARTICLE INFO

Keywords:
Condensed matter physics
Nuclear engineering
Materials science

ABSTRACT

Radiation shielding composites based on polyimide and Bi_2O_3 were synthesized. Surface and physical-mechanical properties of polyimide/Bi_2O_3 composites were studied. Bi_2O_3 particles were modified by polymethylphenylsiloxane for the uniform distribution of filler in composites. This paper presents data on the production of composites in two ways: hot- and cold-pressing. The hot-pressing method for the synthesis of composites is preferable compared to the cold-pressing method (the density increases by 10–12%, and the Vickers microhardness by 10–20%). The results show that the introduction of Bi_2O_3 significantly increases the thermal stability of the composites. At 680 °C, a polymer composite containing 10 wt% Bi_2O_3 retains 9.7% of its mass, and at 60 wt% Bi_2O_3, retains 58.4%. The radiation-protective characteristics of the composites with respect to gamma radiation were evaluated by experimental and theoretical methods. High radiation-protective characteristics of the composites have been established in the gamma-quanta energy range of 0.1–1 MeV.

1. Introduction

The polymer composites are widely used in many industries [1, 2]. The use of polymer composites in space technology reduces the weight of the final products, operating costs, and fuel consumption [3, 4, 5]. However, not all polymers can be used in the harsh conditions of outer space. These conditions include deep vacuum, a sharp temperature drop (from −170 to +200 °C), ionizing radiation, vacuum ultraviolet radiation, micrometeorite particles, atomic oxygen, etc. Under the influence of these conditions, many polymers are destroyed, which leads to a serious violation of their functionalities [6, 7, 8, 9, 10, 11].

PI is one of the few polymers capable of working in the harsh conditions of outer space. PI is used due to its high strength properties, radiation and chemical steadiness, which distinguishes it among heterochain thermoplastics and determines long-term use in space [12, 13, 14].

The use of heavy metal oxides as a filler in a PI matrix can improve the physico-mechanical and radiation-protective characteristics of the material [15, 16, 17]. The selection of appropriate fillers and their concentration can adjust the final properties of the composite [18, 19, 20]. Radiation-protective composites based on PI and heavy metal oxides can be used as a local protection for a spacecraft's electronic equipment. Local protection is an additional screen designed to protect critical nodes and hardware components. The use of such a screen does not entail a serious increase in the mass or dimensions of the spacecraft units and is one of the most effective and cost-effective approaches to ensuring the radiation protection of electronic equipment [21, 22]. The use of such screens allows the use of commercial and industrial class chips instead of radiation-resistant chips, which makes it possible to reduce the price of electronic equipment and expand the range of components used.

In this work, Bi_2O_3 was used as a filler in a PI matrix (modification α-Bi_2O_3). Bismuth oxide is a p-type semiconductor with a high density of 8900 kg/m^3. In contrast to lead, bismuth oxide is non-toxic and has high radiation-protective characteristics with respect to γ-radiation that are almost as good as lead [23]. The use of bismuth oxide as a radiation-protective filler in polymer matrices has been the subject of much research [24, 25, 26]. The article [27] presents data on the introduction of bismuth oxide (up to 60 wt%) to the isophthalic resin. The isophthalic resin/Bi_2O_3 composites have thermal stability up to 200 °C. Verdipoor et al. synthesized radiation-protective composites based on silicone resin and Bi_2O_3 micro and nano-particles. The radiation-protective composites were made of nanoparticles having higher mass attenuation coefficients of γ-radiation relative to those made of microparticles [28]. Kurudirek et al. found that the introduction of Bi_2O_3 into borosilicate glass significantly increased the shielding capability of glassy rays [29].

Abbreviations: PI, polyimide; PMPS, polymethylphenylsiloxane.

* Corresponding author.
E-mail addresses: cherkashina.ni@bstu.ru, natalipv13@mail.ru (N.I. Cherkashina).

https://doi.org/10.1016/j.heliyon.2019.e01703
Received 8 January 2019; Received in revised form 18 March 2019; Accepted 8 May 2019

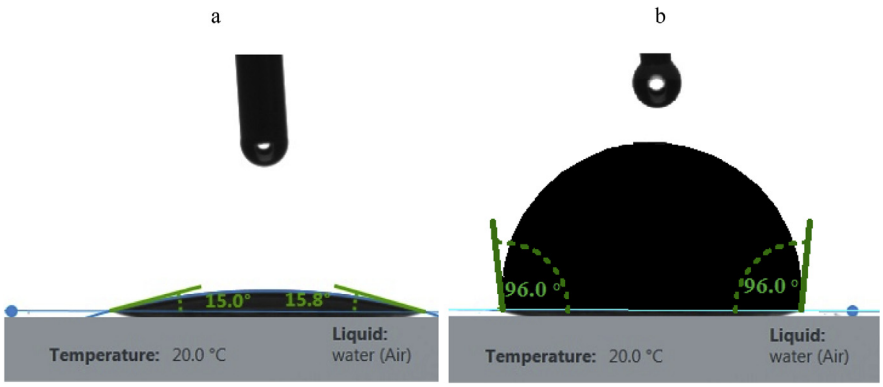

Fig. 1. The image of a water drop on the initial Bi_2O_3 (a) and modified Bi_2O_3 (b).

The introduction of inorganic particles into the organic polymer is associated with a number of technical difficulties, such as aggregation of filler particles and changing the structure of the polymer matrix. To obtain a uniform distribution of inorganic particles in the volume of non-polar polymer matrices, which include PI, fillers are widely modified [30]. Modification is carried out in order to create a hydrophobic particle surface. Studies have shown that surface modification of the inorganic filler leads to an improvement in the mechanical properties of polymer composites [31, 32, 33, 34].

The traditional reagents for the modification of inorganic particles are organosilicon compounds [35]. However, in some cases, it is difficult to obtain a modified carrier with the desired properties (due to the complexity of modifier synthesis, the incompatibility of the necessary functional groups with the anchor grouping, etc.). In recent years, references have appeared in the literature about the possibility of using phosphorus derivatives, such as alkyl phosphonic acids and alkyl phosphates, for modifying the surface of oxides [36, 37]. The chemistry of these compounds is markedly different from the chemistry of organosilicon, so in many cases, they may be useful and even indispensable for obtaining modified surfaces. There are no works on the use of PMPS for the modification of inorganic particles for the purpose of compatibility with PI.

This paper presents data on the synthesis of polymer composites based on a PI matrix and Bi_2O_3 modified with PMPS. Their surface, physico-mechanical and radiation shielding properties were studied.

2. Experimental

2.1. Composites synthesis

PI was used as a matrix for the synthesis of composites in the form of pressed powder (JSC Institute of Plastics named after G.S.Petrov, Moscow, Russia). Bismuth oxide (α-modification) Bi_2O_3 (LLC VitaChem Siberia, Novosibirsk, Russia) was used as a filler. For modifying the filler, a high-temperature PMPS-4 liquid (LLC VitaChem Siberia, Novosibirsk, Russia) was used. The chemical formula of the modifier is $(C_{11}H_8OSi)_n$. PMPS was applied to Bi_2O_3 particles and subjected to further mechanical mixing. The modified Bi_2O_3 was dried at 120 °C for 3 hours. Heat treatment of the modified filler provides chemical fixing and stability of the modification shells. The modifier content was no more than 0.5 wt% of the main mass of Bi_2O_3.

Polymer composites with different contents of Bi_2O_3 were synthesized. For mixing the components, mechanical activation by dispersing in a jet-vortex mill was used. Studies [38, 39, 40] showed that the use of mechanical activation allows the achievement of a uniform distribution of highly dispersed fillers in the polymer matrix. This method activates the surface of the components and makes it possible to avoid aggregation of the filler, retaining the high mechanical characteristics of the polymer composite in a wide temperature range [38, 39, 40].

Composite discs were obtained in two ways. In the first method, the mixture was first pressed and then burned at a temperature of 250–300 °C for 1 hour. In the second method, the mixture was heated to a temperature of 350–400 °C, kept for one hour, and then pressed. After pressing, the polymer composites were cooled to room temperature at a rate of 10 °C/min. The pressing pressure in both cases was the same, 150 MPa. The thickness of the composite discs was 3–5 mm.

2.2. Characterization techniques

Contact-angle measurements were performed at room temperature using a Krüss DSA30 Drop Shape Analysis System.

The size and distribution of particles was measured with ANALYSETTE 22 NanoTecplus (FRITSCH).

Microphotography of Bi_2O_3 and the surface of PI/Bi_2O_3 composite was performed using electronic microscope Tescan Mira 3 LMU.

The density (ρ) of the composites was determined by hydrostatic weighing. First, the mass of the composite was determined in the air, then in a distilled water. After weighing the PI/Bi_2O_3 composites in the air and in the distilled water, ρ was found using formula (1):

$$\rho = \frac{m}{m - m_1} \cdot \rho_w, \tag{1}$$

where m is the mass of the PI/Bi_2O_3 composite in the air; m_1 is the mass of the PI/Bi_2O_3 composite in the distilled water; $\rho_w = 0.998$ g/cm^3.

An STA 449 F1 Jupiter device for synchronous thermal analysis by the company NETZSCH was utilized to carry out the differential thermal analysis.

Microhardness measurement was performed with the use of Duramin-2 microhardness tester. The tester has a range of nine loads, from 98.07 mN (10 g) to 19.61 N (2 kg), which can be selected by the load-interchange mechanism. Loading and un loading of the indenter with the chosen weight occurs automatically with the relevant information displayed on the test er's LCD touchpad.

To study the radiation-protective properties, the PI/Bi_2O_3 composite was irradiated with γ-radiation at an energy of 400 keV and 662 keV. The sources of γ-radiation were radionuclides ^{192}Ir (400 keV) and ^{137}Cs (662 keV). Gamma rays were recorded by the Gamma-beta-spectrometric complex "Progress-BG". The gamma-beta-spectrometric complex error is 5%.

The linear attenuation coefficient (μ) of the composite was found using formula (2):

$$N = N_0 \cdot e^{-\mu \cdot x} \tag{2}$$

where N – the measured count rates in Gamma-beta-spectrometric complex "Progress-BG" with the thickness PI/Bi_2O_3 composite, x (cm); N_0 – the measured count rates in Gamma-beta-spectrometric complex "Progress-BG" without the PI/Bi_2O_3 composite.

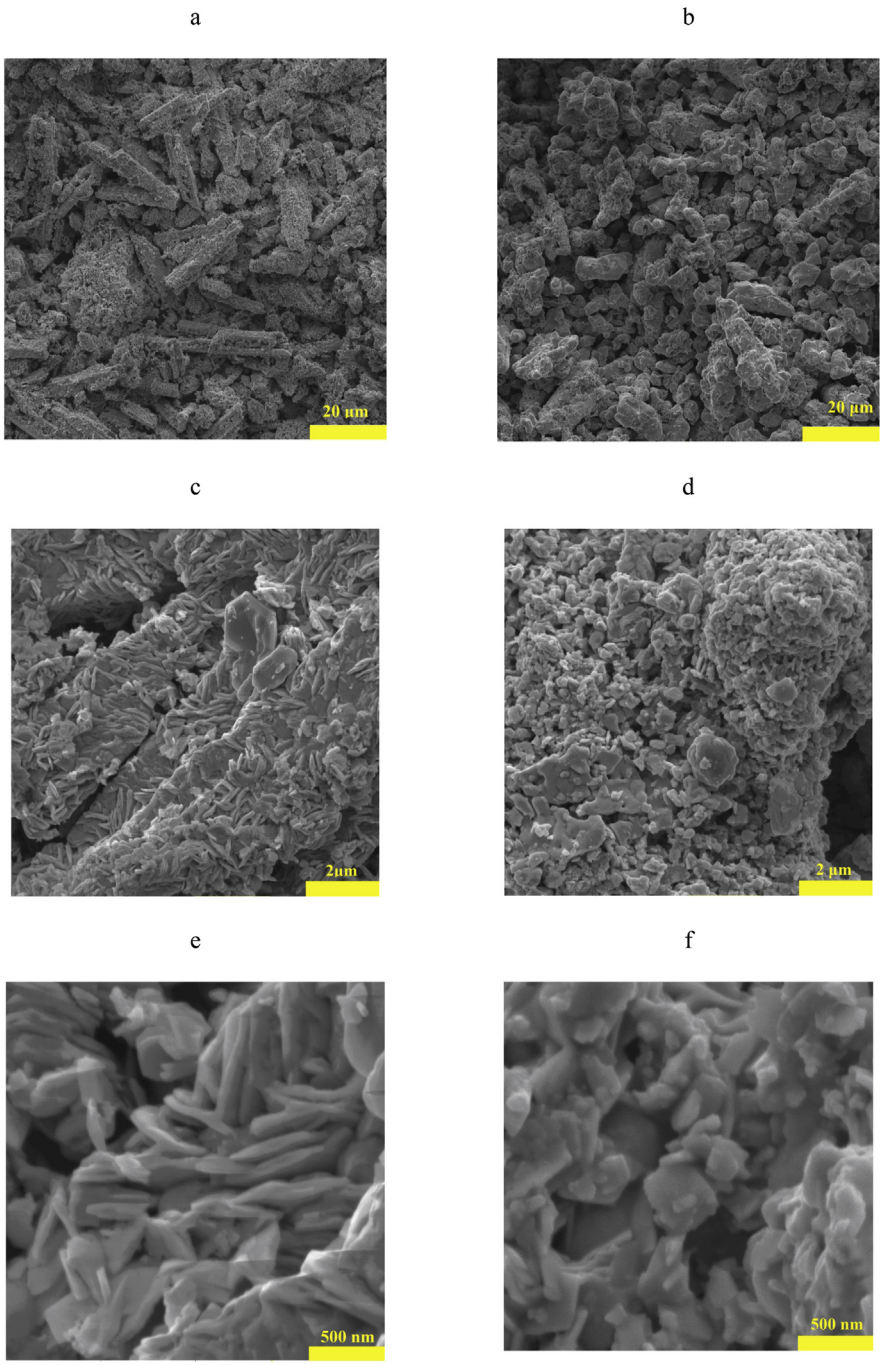

Fig. 2. SEM images of the initial Bi_2O_3 (a,c,e) and modified Bi_2O_3 (b,d,f) at different magnifications.

The mass attenuation coefficient of γ-radiation of the PI/Bi_2O_3 composite was found using formula (3):

$$\mu_m = \mu/\rho \tag{3}$$

The XCOM program was used for a theoretical calculation of the mass attenuation coefficient of the composites. In the XCOM code, the energy range between 1 keV and 100 GeV can be calculated [41].

3. Results and discussion

3.1. Modifying Bi_2O_3

To study the process of modifying Bi_2O_3, tests were performed to determine the contact angle by the method of a spreading drop on the surface of the initial and modified Bi_2O_3. Contact angle θ is a characteristic of the hydrophilicity (hydrophobicity) of the surface of the material. The smaller the angle, the more hydrophilic the surface. Baseline Bi_2O_3 has a hydrophilic surface. The contact angle is 15° (Fig. 1 a). After modifying, the contact angle of Bi_2O_3 is 96° (Fig. 1 b). An increase in the contact angle indicates a positive adsorption of the oligomer (modifier) and its uniform distribution on the outer surface of Bi_2O_3. PMPS liquid imparts a hydrophobic character to the Bi_2O_3 surface, which will allow Bi_2O_3 to evenly distribute throughout the entire volume of the non-polar PI matrix.

Bi_2O_3 is modified via a physical interaction, the procedure involves macromolecules of PMPS adsorbed onto its surface. A polar group of surfactants is adsorbed to the surface of Bi_2O_3 by an electrostatic interaction. As a consequence, the physical attraction between the Bi_2O_3

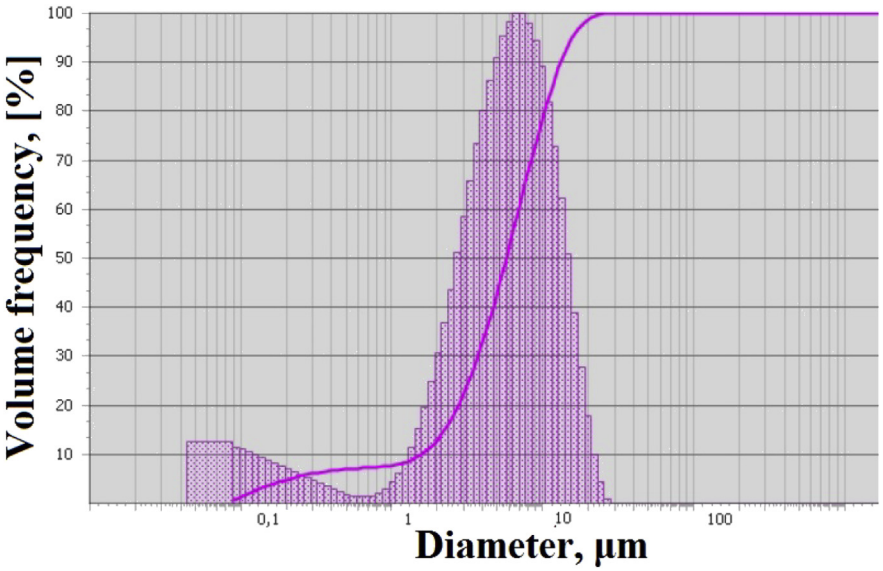

Fig. 3. Particle size distribution of initial Bi_2O_3.

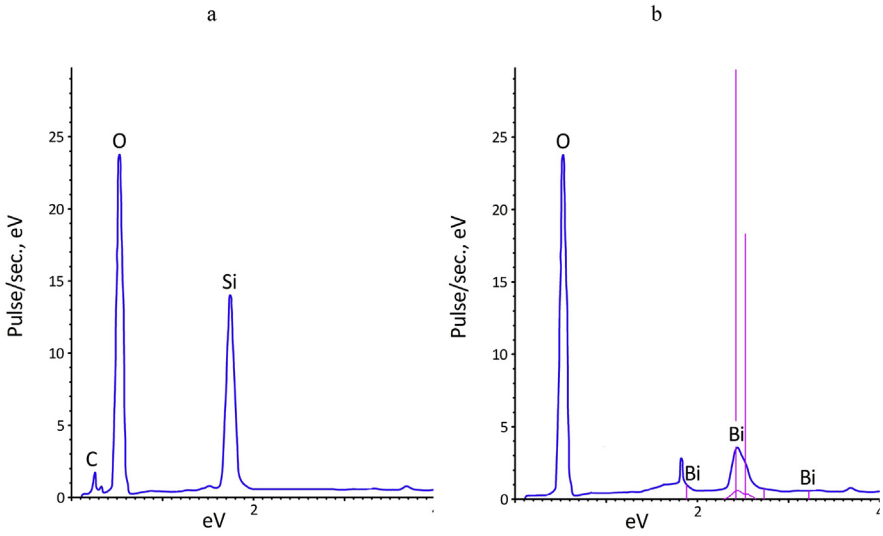

Fig. 4. Electron probe microanalysis of the near-surface (a) and deep (b) layers of modified Bi_2O_3.

particles within agglomerates is reduced, making Bi_2O_3 particles easy to incorporate into a polymer matrix [42].

Fig. 2 shows SEM images of the initial and modified Bi_2O_3 at different magnifications. Microscopic analysis of the original Bi_2O_3 showed that the particles are in the form of long needles. Particle size varies from 2 to 15 µm. What is also confirmed the particle size analyzer results (Fig. 3). The SEM images shows that individual needle particles are combined into large agglomerates with a size of up to 25 µm (Fig. 2 e). Based on the microscopic analysis data the bismuth oxide used is the α-modification, whereas γ-Bi_2O_3 is characterized by non-aggregated crystals of irregular shape, resembling pyramidal and cubic forms [43].

Modifying the surface of Bi_2O_3 leads to a significant change in the microstructure of the particles (Fig. 2 b, d, f). The needle particles present in Fig. 2e disappear after modification. Particles become more rounded with smooth edges. In addition, there is a significant decrease in aggregated Bi_2O_3 particles after modification. Analysis of the microstructure of the modified Bi_2O_3 particle surfaces showed a uniformly formed modification shell on the surface of monodisperse spherical oxide particles. The authors assumed that the obtained powder is Bi_2O_3, the surface of which is coated with PMPS polymerization products. The data obtained from electron probe microanalysis of high-resolution scanning electron microscopy as confirmation of the Bi_2O_3 surface modification. The elemental composition of the Bi_2O_3 of the deep layer (the electron scanning depth in the material at 7 kV does exceed 1 µm) and near-surface layer (the electron scanning depth in the material at 7 kV does not exceed 0.2 µm) are shown in Fig. 4. According to the data obtained, the atomic composition in the near-surface layers of modified Bi_2O_3 shows concentrations of C, O, and Si atoms similar to those present in the composition of PMPS. The presence of Bi in the near-surface layer of modified Bi_2O_3 was not detected.

Table 1
Density of PI/Bi_2O_3 composite obtained by various methods.

Molding method	Density, g/cm^3						
	Bi_2O_3, wt%						
	0	10	20	30	40	50	60
Cold pressing	1.31	1.44	1.60	1.78	2.03	2.32	2.73
Hot pressing	1.43	1.61	1.77	1.99	2.23	2.57	3.05

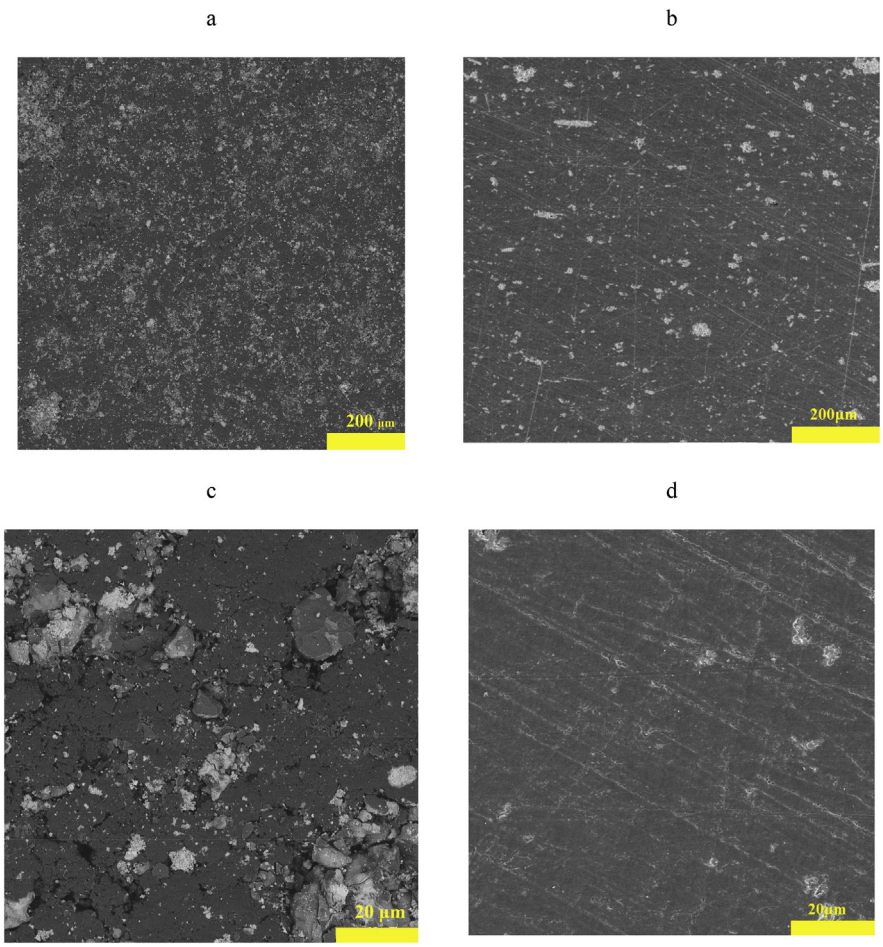

Fig. 5. SEM images of the surface of composites with 50% modified Bi_2O_3 content obtained by cold- (a, c) and hot- (b, d) pressing.

3.2. *Physical-mechanical properties of polyimide/Bi_2O_3 composites*

The synthesis of composite discs was performed in several ways. The first method included cold-pressing with further calcination at a temperature of 250–300 °C for 1 hour. In the second method, hot-pressing was used at a temperature of 350–400 °C and a pressure of 150 MPa. Table 1 presents data on the density of composites obtained by these methods.

Analysis of the data in Table 1 showed that the introduction of a filler leads to an increase in the density of the composites under study, both in the first and second synthesis methods. The composites obtained by hot-pressing have a 10–12% higher density compared with composites obtained by cold-pressing. This is explained by the fact that when using the hot-pressing method, heating the mold and holding at a temperature of 350–400 °C leads to a softening of the PI material and its transition to a viscous-fluid state. Pressing such a viscous-fluid mixture at a pressure of 150 MPa provides high shear deformations, which leads to a uniform distribution of fillers in the polymer melt [44]. In addition, when using such a high specific pressure in the polymer composite, topochemical reactions between its components will occur, which in turn will create a strong connection between them and provide high density and strength characteristics of the developed composite [45].

The physico-mechanical characteristics of compositions based on polymeric materials substantially depend on the homogeneity of the mixtures used. To assess the uniformity of the modified Bi_2O_3 distribution in the volume of the PI matrix, the microstructure of the obtained composite surfaces was studied. Fig. 5 shows SEM images of the composite surfaces with 50% modified Bi_2O_3 content obtained by cold- and hot-pressing. Analysis of the composite surface microstructure obtained by both methods showed a fine-grained structure.

Table 2
Vickers microhardness (HV) for composites obtained by various methods.

Molding method	Vickers microhardness (HV)						
	Bi_2O_3, wt%						
	0	10	20	30	40	50	60
Cold pressing	42.2	48.3	57.2	62.9	66.9	73.0	76.6
Hot pressing	50.3	58.9	65.8	71.5	78.7	84.9	90.1

However, the surface of the composite obtained by cold-pressing has a loose structure with a large number of pores (Fig. 5a, c). The particles of modified Bi_2O_3 are non-uniformly distributed in the PI matrix due to the high aggregation of the particles. In spite of this, no microcracks or shells were observed on the surface of the composite obtained by cold-pressing. The composite produced by hot-pressing has a dense structure. Individual isolated pores were observed in the field of large filler particles.

To analyze the influence of the pressing method on the packing density, surface structure, and thin surface layers of composites, the microhardness of the material surface was studied. The hardness of the material means its resistance to local plastic deformation when another body, which is not subject to such deformation, penetrates it. When evaluating the Vickers microhardness, a pyramidal diamond indenter was pressed into the surface of the composites under a load acting for a fixed time (not less than 15 sec.). The load in all dimensions was the same, 200 g Table 2 presents data on Vickers microhardness for composites obtained by cold- and hot-pressing.

Analysis of the data in Table 2 showed that the introduction of Bi_2O_3

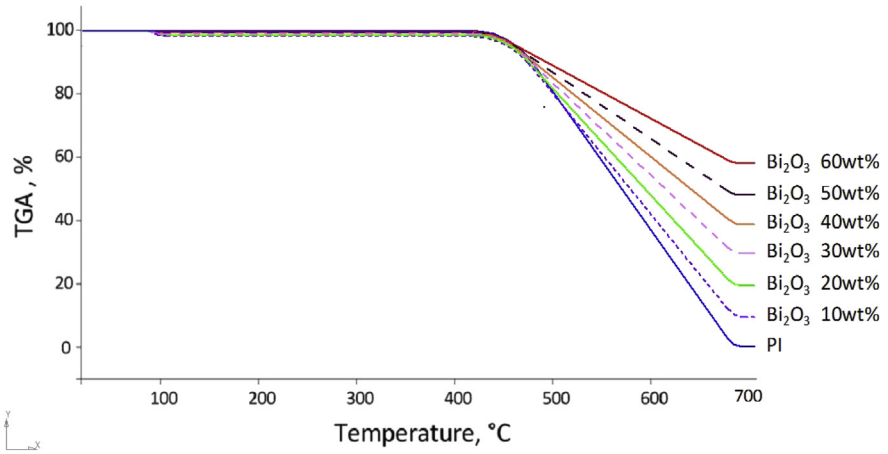

Fig. 6. TGA curves for pure PI and PI/Bi_2O_3 composite.

Table 3
Weight level in PI/Bi_2O_3 composite samples.

Temperature (°C)	Weight level, %						
	Bi_2O_3, wt%						
	0	10	20	30	40	50	60
450	97.3	97.3	97.3	97.3	97.3	97.3	97.3
500	96.5	96.5	96.5	96.5	96.5	96.5	96.5
550	89.9	90.6	91.4	92.1	92.8	93.6	94.3
600	56.6	60.7	64.7	68.8	72.8	76.9	80.9
680	0	9.7	19.4	29.2	38.9	48.6	58.4

filler significantly increases the microhardness of the composites, higher Bi_2O_3 content corresponds to higher Vickers microhardness. This is true for composites obtained by both cold- and hot-pressing. The increase in Vickers microhardness with increasing filler content is due to the fact that Bi_2O_3 has a harder surface. The hardness of Bi_2O_3 on the Mohs scale is 4–5 [46], while the hardness for PI on the Mohs scale is only 1 [47]. In [48, 49], it was shown that the introduction of inorganic particles significantly increases the microhardness of polymer composites.

As can be seen in Table 2, the Vickers microhardness strongly depends on the method of synthesis of the composite. When using the hot-pressing method, the Vickers microhardness is 10–20% more for composites made by cold-pressing for the same composition. This is consistent with the SEM images data of the composite surfaces. The looser surface structure obtained by cold-pressing will have a lower microhardness (Fig. 5 a, c). The more dense structure with a maximum degree of packing and minimal porosity (Fig. 5 b, d) obtained by hot pressing will have a high microhardness. The strong variation in microhardness, by 10–20%, with the use of various methods for the synthesis of composites is also related to the high error of the instrument used in measuring Vickers microhardness.

Based on the obtained data on density, surface microstructure and microhardness, the hot-pressing method for the synthesis of composites is preferable. The hot pressing method allows more dense composites to be obtained, which will lead to a significant increase in their physico-mechanical characteristics.

To reveal the influence of the filler on the heat resistance of the obtained composites, a thermogravimetric analysis of composites with different Bi_2O_3 contents was carried out. Thermogravimetric analysis is a method of studying physico-chemical and chemical processes and reactions based on recording the thermal effects (enthalpy changes) accompanying the transformations of substances under temperature programming conditions [50]. The study of thermal characteristics was carried out in the range from 20–700 °C. Fig. 6 shows the TGA curves of pure PI and composites containing up to 60% wt. modified Bi_2O_3. Fig. 6 shows that pure PI is stable to 425.6 °C, without loss of mass on the TGA curve. At a temperature of 680 °C, complete thermal decomposition of

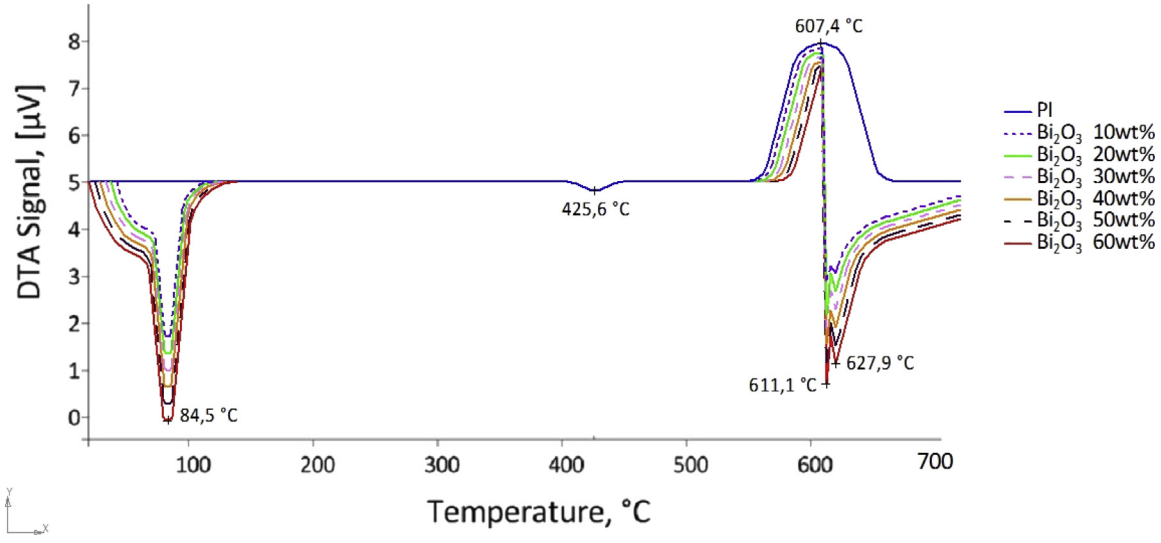

Fig. 7. DTA curves for pure PI and PI/Bi_2O_3 composite.

Table 4
Elemental atomic composition of the composites under study.

Bi_2O_3, wt%	Atom content, wt%				
	C	N	O	H	Bi
0	68.11	7.57	21.62	2.70	-
10	61.30	6.81	20.49	2.43	8.97
20	54.49	6.05	19.36	2.16	17.94
30	47.68	5.30	18.22	1.89	26.91
40	40.86	4.55	17.09	1.62	35.88
50	34.06	3.78	15.96	1.35	44.85
60	27.24	3.03	14.83	1.08	53.82

the PI occurs. The results obtained for the thermal stability of PI are consistent with the literature data [51, 52]. It is known that the introduction of inorganic filler significantly increases the thermal stability of polymers [53, 54, 55]. This is clearly seen in Fig. 5; as the content of Bi_2O_3 increases, the rate of mass loss for the composite decreases. However, a slight mass loss in composites begins at an 80–120 °C, which is most likely due to the loss of sorbed and hydroxyl water contained in Bi_2O_3 [56]. Table 3 presents data on the thermal stability of the composites.

Data of Fig. 6 and Table 3 shows that the thermal stability of the PI less than the PI/Bi_2O_3 composites. It's known that thermal stability of the inorganic compounds is greater than thermal stability of polymers [57, 58].

Fig. 7 shows the DTA curves of PI and PI/Bi_2O_3 composite samples. The DTA curve of pure PI is characterized by a long exo-effect with a marked maximum at 670°C, corresponding to the maximum decomposition rate of the PI. Also on the DTA curve of pure PI, there is a small endothermic peak at 425.6 °C. On the TGA curve, this temperature corresponds to the beginning of the thermal degradation of the PI. In addition, several pronounced peaks appear on the DTA curves of the composites. The endo-effect at 84.5 °C in the low-temperature range (80–120 °C), accompanied by a change in the mass of the samples, was related to the loss of sorbed and hydroxyl water in Bi_2O_3. Also, the DTA curves of composites are characterized by an extended endo-effect with marked maxima at 611.1 and 627.9°C. This endothermic effect appears to be due to recrystallization of Bi_2O_3 [56].

3.3. Radiation shielding properties of polyimide/Bi_2O_3 composites

Evaluation of the radiation shielding properties of polyimide/Bi_2O_3 composites with respect to gamma radiation were estimated by the data of the mass attenuation coefficient of γ-radiation (μ_m). The mass attenuation coefficient of γ-radiation was calculated experimentally and theoretically using the XCOM program. This program allows you to calculate the gamma radiation attenuation coefficients for mixed substances, depending on their chemical (atomic) composition. Table 4 presents the elemental atomic chemical composition of the composites under study.

Fig. 8 shows the curves of the dependence of the gamma radiation mass attenuation coefficient as a function of the energy of gamma rays. The energy of gamma rays ranged from 0.1–1 MeV. As expected, with an

Table 5
Mass attenuation coefficient of γ-radiation (μ_m) PI/Bi_2O_3 composite samples.

Bi_2O_3 wt%	μ_m, cm^2/g			
	E, keV			
	400		662	
	XCOM program	Experiment	XCOM program	Experiment
0	0.11	0.12 ± 0.01	0.08	0.08 ± 0.01
10	0.26	0.27 ± 0.03	0.11	0.13 ± 0.01
20	0.38	0.38 ± 0.03	0.13	0.15 ± 0.02
30	0.49	0.50 ± 0.04	0.17	0.16 ± 0.01
40	0.57	0.53 ± 0.06	0.19	0.21 ± 0.03
50	0.68	0.64 ± 0.06	0.21	0.23 ± 0.03
60	0.75	0.76 ± 0.07	0.22	0.24 ± 0.03

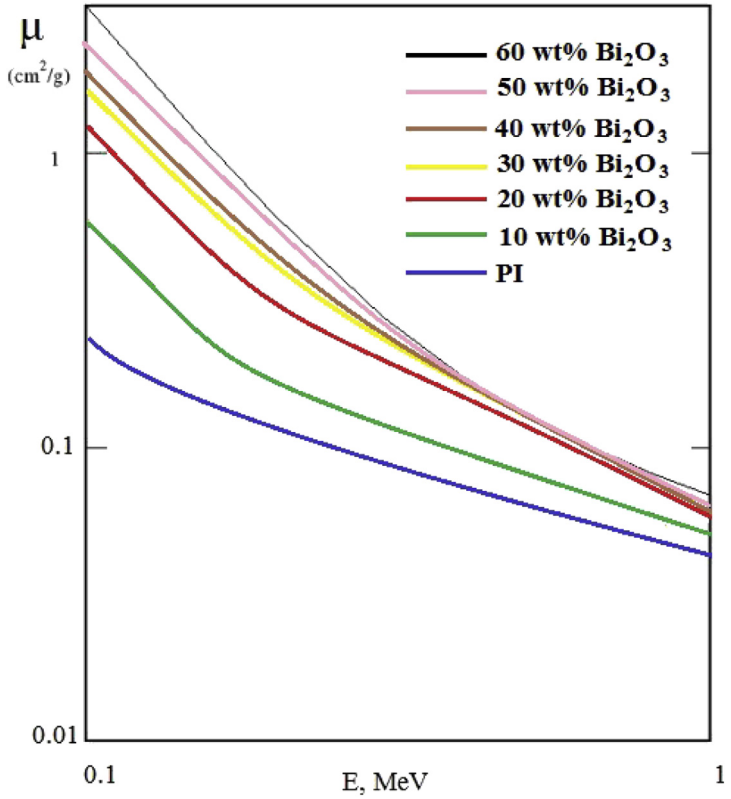

Fig. 8. Curves of the mass attenuation coefficient of gamma radiation of composites as a function of energy.

increase in the content of Bi_2O_3, an increase in the mass attenuation coefficient was observed in the entire investigated energy range. The curves are linear in nature and are located one below the other.

Table 5 presents a data of mass attenuation coefficient of γ-radiation PI/Bi_2O_3 composite samples, based on calculated and experimental data at the same effective γ-radiation energy (400 keV and 662 keV). The experimental values accounted for the error of the Gamma-beta-spectrometric complex "Progress-BG" (5%).

Table 5 shows high accuracy of the mass attenuation coefficient of γ-radiation calculated with the XCOM program, and experimental data obtained with of the Gamma-beta-spectrometric complex "Progress-BG". The difference between μm which is calculated in the XCOM program and μm which is obtained with of the Gamma-beta-spectrometric complex "Progress-BG" was around 7–12% (the largest and smallest values were taken into account taking into account the measurement error).

4. Conclusions

It is shown that the modification of Bi_2O_3 with PMPS fluid makes the surface of the filler hydrophobic. The uniformly formed modification shell on the surface of monodisperse spherical Bi_2O_3 particles has been established.

When using the hot-pressing method, the Vickers microhardness is 10–20% more than composites obtained by cold-pressing, for the same composition. The introduction of Bi_2O_3 significantly increases the thermal stability of composites. At 680 °C, a polymer composite containing 10 wt% Bi_2O_3 retains 9.7% of its mass, and at 60 wt% Bi_2O_3, retains 58.4%.

High radiation-protective characteristics with respect to gamma radiation, in the 0.1–1 MeV range, for the composites have been established by theoretical and experimental methods.

Declarations

Author contribution statement

Vyacheslav I. Pavlenko: Conceived and designed the experiments; Analyzed and interpreted the data; Contributed reagents, materials, analysis tools or data.

Natalia I. Cherkashina: Conceived and designed the experiments; Performed the experiments; Analyzed and interpreted the data; Contributed reagents, materials, analysis tools or data; Wrote the paper.

Roman N. Yastrebinsky: Performed the experiments; Analyzed and interpreted the data; Contributed reagents, materials, analysis tools or data.

Funding statement

This work was supported by the Base University on the basis of BSTU named after V. G. Shukhov [grant number A-82/17].

Competing interest statement

The authors declare no conflict of interest.

Additional information

No additional information is available for this paper.

References

[1] M. Lim, H. Kwon, D. Kim, J. Seo, H. Han, S.B. Khan, Highly-enhanced water resistant and oxygen barrier properties of cross-linked poly(vinyl alcohol) hybrid films for packaging applications, Prog. Org. Coating 85 (2015) 68–75.

[2] E.S. Jang, S.B. Khan, J. Seo, Y.H. Nam, W.J. Choi, K. Akhtar, H. Han, Synthesis and characterization of novel UV-curable polyurethane–clay nanohybrid: influence of organically modified layered silicates on the properties of polyurethane, Prog. Org. Coating 71 (2011) 36–42.

[3] T. Zaigham, Space applications of composite materials, J. Spacecr. Technol. 08 (2018) 65–70.

[4] S. Chen, S. Nambiar, Z. Li, Y. Sun, S. Gong, G.Z.H. Zhu, J.T.W. Yeow, Polymer Nanocomposite for Space Applications, in: 14th IEEE International Conference on Nanotechnology, Toronto, ON, 2014, pp. 685–688.

[5] A.G. Koniuszewska, J.W. Kaczmar, Application of polymer based composite materials in transportation, Prog. Rubber Plast. Recycl. Technol. 32 (2016) 1–24.

[6] S.W. Samwel, Low earth orbital atomic oxygen erosion effect on spacecraft materials, Space Res. J. 7 (2014) 1–13.

[7] V.A. Shuvalov, G.S. Kochubei, A.I. Priimak, N.I. Pismennyi, N.A. Tokmak, Changes of properties of the materials of spacecraft solar arrays under the action of atomic oxygen, Cosmic Res. 45 (2007) 294–304.

[8] L. Singh, K.S. Samra, Opto-structural characterization of proton (3 MeV) irradiated polycarbonate and polystyrene, Radiat. Phys. Chem. 77 (2008) 252–258.

[9] A.I. Wozniak, V.S. Ivanov, O.A. Zhdanovich, V.I. Nazarov, A.S. Yegorov, Modern approaches to polymer materials protecting from ionizing radiation, Orient. J. Chem. 33 (2017) 2148–2163.

[10] V.I. Pavlenko, N.I. Cherkashina, Effect of SiO_2 crystal structure on the stability of polymer composites exposed to vacuum ultraviolet radiation, Acta Astronaut. 155 (2019) 1–9.

[11] V.I. Pavlenko, N.I. Cherkashina, O.D. Edamenko, V.T. Zabolotny, Effect of vacuum ultraviolet on the surface properties of high-filled polymer composites, Inorg. Mater.: Appl. Res. 5 (2014) 219–223.

[12] X. Fang, Z. Yang, S. Zhang, L. Gao, M. Ding, Synthesis and properties of polyimides derived from cis- and trans-1,2,3,4-cyclohexanetetracarboxylic dianhydrides, Polym 45 (2004) 2539–2549.

[13] S. Xie, Z. Zhang, W. Wei, Synthesis and properties of polyimide-based optical materials, J. Korean Phys. Soc. 51 (2007) 1536–1541.

[14] C. Qu, J. Hu, X. Liu, Z. Li, Y. Ding, Morphology and mechanical properties of polyimide films: the effects of UV irradiation on microscale surface, Materials (Basel) 10 (2017) pii: E1329.

[15] S.B. Khan, K.A. Alamry, H.M. Marwani, A.M. Asiri, M.M. Rahman, Synthesis and environmental applications of cellulose/ZrO_2 nanohybrid as a selective adsorbent for nickel ion, Comp. Part B-Eng. 50 (2013) 253–258.

[16] E.S. Jang, S.B. Khan, J. Seo, K. Akhtar, J. Choi, K.I. Kim, H. Han, Synthesis and characterization of novel UV-Curable PU-Si hybrids: Influence of silica on thermal, mechanical, and water sorption properties of polyurethane acrylates, Macromol. Res. 19 (2011) 1006.

[17] S.B. Khan, K.A. Alamry, E.N. Bifari, A.M. Asiri, M. Yasir, L. Gzara, R.Z. Ahmad, Assessment of antibacterial cellulose nanocomposites for water permeability and salt rejection, J. Ind. Eng. Chem. 24 (2015) 266–275.

[18] F.P. Cota, R.A.A. Alves, T.H. Panzera, K. Strecker, A.L. Christoforo, P.H.R. Borges, Physical properties and microstructure of ceramic–polymer composites for restoration works, Mat. Sci. Eng. A-Struct. 531 (2012) 28–34.

[19] P.D. Bloom, K.G. Baikerikar, J.U. Otaigbe, V.V. Sheares, Development of novel polymer/quasicrystal composite materials, Mat. Sci. Eng. A-Struct. 294–296 (2000) 156–159.

[20] A.A. Arbuzova, M.A. Votyakov, Estimation of the influence of the state of the reinforcing polymer in the structure of polymeric fiber material using mathematical prediction methods, Chem. Bull. 1 (2018) 12–17.

[21] F.E. Vilkov, A.A. Lozovan, A.V. Bazhanov, A.N. Kasitsyn, O.E. Schekoturova, M.K. Solovev, Investigation of the radiation-protective properties of a highly filled liquid glass material, J. Surface Invest.: X-Ray, Synchrotron Neutron Tech. 11 (2017) 912–916.

[22] F.S. Pellicori, C.L. Martinez, P. Hausgen, D. Wilt, Development and testing of coatings for orbital space radiation environments, Appl. Opt. 53 (2014) A339–A350.

[23] H. Shirkhanloo, M. Saffari, S.M. Amini, M. Rashidi, Novel semisolid design based on bismuth oxide (Bi_2O_3) nanoparticles for radiation protection, Nanomed. Res. J. 4 (2017) 230–238.

[24] M. Dejangah, M. Ghojavand, R. Poursalehi, P.R. Gholipour, Study gamma radiation protection properties of silicon rubber-bismuth oxide nanocomposites: synthesis, characterization and simulation, Iran, J. Radiat. Safety Meas. 4 (2016) 37–46.

[25] T. Özdemir, Monte Carlo simulations of radioactive waste encapsulated by bisphenol-A polycarbonate and effect of bismuth-III oxide filler material, Radiat. Phys. Chem. 135 (2017) 11–17.

[26] V.I. Pavlenko, D.G. Tarasov, O.D. Edamenko, G.G. Bondarenko, Gamma modification of radiation-resistant fluoroplastic composite, Inorg. Mater.: Appl. Res. 4 (2013) 389–393.

[27] M.R. Ambika, N. Nagaiah, V. Harish, N.K. Lokanath, M.A. Sridhar, N.M. Renukappa, S.K. Suman, Preparation and characterisation of Isophthalic-Bi_2O_3 polymer composite gamma radiation shields, Radiat. Phys. Chem. 130 (2017) 351–358.

[28] K. Verdipoor, A. Alemi, A. Mesbahi, Photon mass attenuation coefficients of a silicon resin loaded with WO_3, PbO, and Bi_2O_3 Micro and Nano-particles for radiation shielding, Radiat. Phys. Chem. 147 (2018) 85–90.

[29] M. Kurudirek, N. Chutithanapanon, R. Laopaiboon, C. Yenchai, C. Bootjomchai, Effect of Bi_2O_3 on gamma ray shielding and structural properties of borosilicate glasses recycled from high pressure sodium lamp glass, J. Alloy. Comp. 745 (2018) 355–364.

[30] X. Hou, F. Zhou, B. Yu, We. Liu, Superhydrophobic zinc oxide surface by differential etching and hydrophobic modification, Mat. Sci. Eng. A-Struct. 452–453 (2007) 732–736.

[31] Y. Qi, B. Xiang, W. Tan, J. Zhang, Hydrophobic surface modification of TiO_2 nanoparticles for production of acrylonitrile-styrene-acrylate terpolymer/TiO_2 composited cool materials, Appl. Surf. Sci. 419 (2017) 213–223.

[32] V.I. Pavlenko, N.I. Cherkashina, Synthesis of hydrophobic filler for polymer composites, Int. J. Eng. Technol. 2 (23) (2018) 493–495.
[33] M.Z. Rong, M.Q. Zhang, W.H. Ruan, Surface modification of nanoscale fillers for improving properties of polymer nanocomposites: a review, Mater. Sci. Tech-Lond. 22 (2006) 787–796.
[34] Y.H. Lai, M.C. Kuo, J.C. Huang, M. Chen, On the PEEK composites reinforced by surface-modified nano-silica, Mat. Sci. Eng. A-Struct. 458 (2007) 158–169.
[35] H. Maciejewski, J. Karasiewicz, M. Dutkiewicz, M. Nowicki, L. Majchrzycki, Effect of the type of fluorofunctional organosilicon compounds and the method of their application onto the surface on its hydrophobic properties, RSC Adv. 4 (2014) 52668–52675.
[36] C. Queffélec, M. Petit, P. Janvier, D.A. Knight, B. Bujoli, Surface modification using phosphonic acids and esters, Chem. Rev. 112 (2012) 3777–3807.
[37] R. Hofer, M. Textor, N. Spencer, Alkyl phosphate monolayers, self-assembled from aqueous solution onto metal oxide surfaces, Langmuir 17 (2001) 4014–4020.
[38] T.A. Xavier, N.R.G. Fróes-Salgado, M.M. Meier, R.R. Braga, Influence of silane content and filler distribution on chemical-mechanical properties of resin composites, Braz. Oral Res. 29 (2015) 1–8.
[39] H.O. Sirenko, L.M. Soltys, I.V. Sulyma, M.I. Martynyuk, Methods of thermochemical and mechanical activation of fillers of polymer composite materials, Phys. Chem. Solid State 18 (2017) 249–251.
[40] U. Ziyamukhamedova, D. Djumabaev, B. Shaymardanov, Mechanochemical modification method used in the development of new composite materials based on epoxy binder and natural minerals, Turk. J. Chem. 37 (2013) 51–56.
[41] M.J. Berger, J.H. Hubbell, S.M. Seltzer, J. Chang, J.S. Coursey, et al., XCOM: Photon Cross Sections, NIST Standard Reference Database, XGAM), 2010.
[42] M. Conradi, Nanosilica-reinforced polymer composites, Materiali in tehnologije/ Mater. Technol. 47 (2013) 285–293.
[43] A.V. Egorysheva, O.M. Gaitko, T.B. Kuvshinova, S.V. Golodukhina, V.A. Lebedev, Kh.E. Erov, Targeted synthesis ultrafine α- and γ-Bi_2O_3 having different morphologies, Russ. J. Inorg. Chem. 62 (2017) 1426–1434.
[44] P.R. Hornsby, Compounding of particulate-filled thermoplastics, in: S. Palsule (Ed.), Encyclopedia of Polymers and Composites, Springer, Berlin, Heidelberg, 2013.
[45] P. Thomas, B.S. Dakshayini, H.S. Kushwaha, R. Vaish, Effect of Sr_2TiMnO_6 fillers on mechanical, dielectric and thermal behaviour of PMMA polymer, J. Adv. Dielectric. 5 (2015) 1550018.
[46] M.K. Trivedi, R.M. Tallapragada, A. Branton, D. Trivedi, G. Nayak, Evaluation of atomic, physical, and thermal properties of bismuth oxide powder: an impact of biofield energy treatment, American J. Nano Res. Appl. 6 (2015) 94–98.
[47] J.W. Gooc, Mohs hardness, in: J.W. Gooch (Ed.), Encyclopedic Dictionary of Polymers, Springer, New York, NY, 2011.
[48] E.G. Mota, A. Weiss, A.M. Spohr, H.M.S. Oshima, L.M.N. de Carvalho, Relationship between filler content and selected mechanical properties of six microhybrid composites, Rev. Odonto Ciência 26 (2011) 151–155.
[49] D. Pieniak, A. Walczak, A.M. Niewczas, Comparative study of wear resistance of the composite with microhybrid structure and nanocomposite, Acta Mech. Automatica 10 (2016) 306–309.
[50] R.V. Rodrigues, E.J.B. Muri, P.C.M. da Cruz, A.A.L. Marins, L.U. Khan, R.M. Oliveira, J.R. Matos, H.F. Brito, L.C. Machado, Thermogravimetric study on preparation of NiTiO3 in different reaction times, J. Therm. Anal. Calorim. 126 (2016) 1499–1505.
[51] M.B. Ahmad, Y. Gharayebi, M.S. Salit, M.Z. Hussein, S. Ebrahimiasl, A. Dehzangi, Preparation, characterization and thermal degradation of polyimide (4-APS/ BTDA)/SiO_2 composite films, Int. J. Mol. Sci. 13 (2012) 4860–4872.
[52] T.H. Johnston, C.A. Gaulin, Thermal decomposition of polyimides in vacuum, J. Macromol. Sci. A. 6 (1969) 1161–1182.
[53] J.M. Hwu, G.J. Jiang, Z.M. Gao, W. Xie, W.P. Pan, The characterization of organic modified clay and clay-filled PMMA nanocomposite, J. Appl. Polym. Sci. 83 (2002) 1702–1710.
[54] M.E. Achour, A. Droussi, D. Medine, A. Oueriagli, A. Outzourhit, A. Belhadj Mohamed, H. Zangar, Thermal and dielectric properties of polypyrrolepoly (methyl methacrylate) nanocomposites, Int. J. Phys. Sci. 6 (2011) 5075–5079.
[55] N.I. Cherkashina, A.V. Pavlenko, Synthesis of polymer composite based on polyimide and $Bi_{12}SiO_{20}$ sillenite, Polym. Plast. Technol. Eng. (2018) 1–9.
[56] L.A. Klinkova, V.I. Nikolaichik, N.V. Barkovskii, V.K. Fedotov, Thermal stability of Bi_2O_3, Russ. J. Inorg. Chem. 52 (2007) 1822–1829.
[57] M.Q. Liu, J.P. Duan, X.Z. Shi, J.J. Lu, W. Huang, Thermo-stabilized, porous polyimide microspheres prepared from nanosized SiO_2 templating via in situ polymerization, Express Polym. Lett. 9 (2015) 14–22.
[58] X.-Y. Shang, Z.-K. Zhu, J. Yin, X.-D. Ma, Compatibility of soluble polyimide/silica hybrids induced by a coupling agent, Chem. Mater. 14 (2002) 71–77.